

# Boiler flame detection algorithm based on PSO-RBF network<sup>①</sup>

WU Jin(吴进)<sup>②</sup>, GAO Yaqiong, YANG Ling, ZHAO Bo

(School of Electronic Engineering, Xi'an University of Posts and Telecommunications, Xi'an 710121, P. R. China)

## Abstract

As the main production tool in the industrial environment, large boilers play a vital role in the conversion and utilization of energy. Therefore, the furnace flame detection technology for boilers has always been a hot issue in the field of industrial automation and intelligence. In order to further improve the timeliness and accuracy of the flame detection network, a radial basis function (RBF) flame detection network based on particle swarm optimization (PSO) algorithm is proposed. First, the proposed algorithm initializes the speed and position parameters of the particles. Then, the parameters of the particles are mapped to the RBF flame detection network. Finally, the algorithm is iteratively updated to obtain the global optimal solution. The PSO-RBF flame detection algorithm adopts a flame sample collection method similar to back propagation (BP) flame detection algorithm, and further improves the collection efficiency. The experimental results show that the PSO-RBF flame detection network has good accuracy and faster convergence speed in the given data samples. In the flame data samples, the detection accuracy of the PSO-RBF flame detection algorithm reaches 90.5%.

**Key words:** radial basis function(RBF), particle swarm optimization(PSO), flame detection

## 0 Introduction

In today's industrial environment, boilers are widely used, and large boilers, as the main production tool, still play a vital role in energy conversion and utilization<sup>[1]</sup>. The results of the flame state judgment and the subsequent fuel supply in the furnace are directly affected by the accuracy of the detection method, which will affect the utilization rate of primary energy of large boilers to a large extent. The fuel combustion condition in the boiler furnace directly determines the safety and stability of the boiler operation and the entire industrial production<sup>[2]</sup>. The safety of industrial boiler operation is indispensable to furnace flame detection<sup>[3-4]</sup>.

According to the current research results of the flame detection problem of large industrial boilers and the flame detection technology currently put into production, the flame detection methods of boiler furnaces can be roughly divided into the following four categories: sensor measurement method<sup>[5]</sup>, digital signal processing method<sup>[6]</sup>, image processing method<sup>[7]</sup>, machine learning method<sup>[8]</sup>. Flame detection systems based on various types of sensors and traditional digital signal

processing methods often need to adjust the accuracy of the sensor according to requirements during industrial production. However, it is difficult to configure the flame sensor to achieve accurate detection in practice<sup>[9]</sup>. In addition, conventional flame detection sensing devices do not define the main characteristics of the flame very well<sup>[10]</sup>. The use of charge coupled device (CCD) indirect measurement cannot effectively detect flames visually. In view of the low accuracy of the existing boiler flame detection technology, some researchers have explored the feasibility and potential advantages of neural network in flame detection, used furnace data and boiler operating parameters for training, and established a neural network to determine the output water temperature of the boiler system, so as to analyze the heat output and flame state of the boiler<sup>[11]</sup>. Aiming at the problems of diverse flame shapes and unclear edges, Li et al.<sup>[12]</sup> proposed a proposal mechanism method based on two key attributes of flame dynamics and color to effectively select candidate flame regions. And based on the processed images, convolutional neural network (CNN) framework for the flame region was proposed. Chao et al.<sup>[13]</sup> improved a flame detection method based on faster R-CNN network to identify and judge flames, and the model accuracy rate

① Supported by Shaanxi Province Key Research and Development Project (No. 2021GY-280, 2021GY-029), Shaanxi Province Natural Science Basic Research Program Project (No. 2021JM-459) and National Natural Science Foundation of China (No. 61834005, 61772417, 61802304).

② To whom correspondence should be addressed. E-mail: wujin1026@126.com.

Received on June 7, 2022

reached more than 85%. Lv et al.<sup>[14]</sup> proposed a detection model that combines CNNs and long short-term Memory (LSTM) networks, and the results show that flame images can be correctly identified. Yu and Chen<sup>[15]</sup> proposed a video flame detection method based on the combination of dual-stream convolutional neural network and spatiotemporal features. Aslan et al.<sup>[16]</sup> proposed a vision-based approach that uses deep convolutional generation adversarial neural (DCGAN) networks to detect flames and performs effective detection.

To sum up, the existing flame detection algorithms have slow convergence speed, long running time, low detection accuracy, and it is difficult to ensure the timeliness of practical applications. Therefore, this paper proposes a flame detection algorithm based on particle swarm optimization-radial basis function (PSO-RBF) network. The RBF flame detection network structure is designed and PSO algorithm is further used to optimize the network. Through the iterative update of the network, the global optimal solution is obtained and the network model is constructed. The flame sample data is obtained after feature extraction, area calculation, and frequency extraction of the original flame image using image processing algorithms, which are used as the training and testing samples of the PSO-RBF neural network. Through the detection experiment of the flame state and smoke state in the furnace through the PSO-RBF network, the feasibility of the flame detection algorithm described in this paper is verified, which can basically meet the needs of industrial boiler production.

## 1 PSO-RBF flame detection network design

### 1.1 RBF flame detection network model

The RBF neural network method for multivariate interpolation is a feedforward neural network, and RBF network is designed by imitating the neural network distribution structure in the human brain<sup>[17]</sup>. It can be seen from the network structure that RBF neural network and human brain neural network have the following remarkable characteristics: each neuron covers each other to achieve transmission and reception, and each parameter transmission only needs to be adjusted locally to achieve optimization. Due to the simple structure of RBF network, the operating efficiency of the algorithm has a significant speed advantage compared with other machine learning algorithms, so the application of the RBF network is also very extensive.

At present, deep learning algorithms are used in models for furnace flame detection, the use of back

propagation (BP) neural network to achieve detection has certain advantages, but due to the more or less algorithm limitations of BP flame detection algorithm, for example, the adjustment of weights adopts negative gradient descent. This method of adjusting the weights will reduce the operating efficiency of the algorithm, that is, there are disadvantages such as slow convergence speed, long training time, and ease to fall into local minima<sup>[18]</sup>.

Therefore, combining the excellent approximation performance of the RBF network in the feedforward neural network, the ease of finding the global optimal solution, and the fast learning speed of the network, it can be used in industrial furnace flame detection, which can improve the timeliness of the algorithm.

As shown in Fig. 1, the RBF network model designed and used in this paper consists of three layers. Only the input signal is propagated between the input node and the hidden layer, and the basis function contained in the hidden layer node is called the function function of the network, also known as the action function; the signal of the input layer is approximated locally, and the basis function of the hidden layer will generate a response locally in the function, which is called the local adjustment response.

In Fig. 1,  $i$  represents the number of nodes in any layer,  $x_i$  is the node of the input layer,  $R_i(x)$  represents the hidden layer node that selects the Gaussian function as the basis function, and  $F_i(x)$  is the output layer parameter. Set the number of centers.

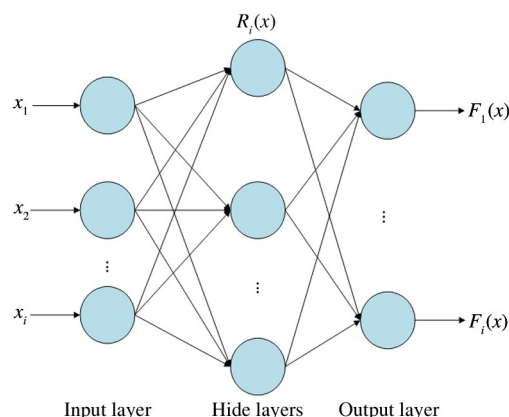


Fig. 1 RBF network topology diagram

### 1.2 PSO improves RBF flame detection network

The proposal of PSO algorithm is obtained by observing the foraging behavior of birds. The proposal of PSO algorithm can effectively solve the shortcomings of the swarm intelligence optimization algorithm. For example, most optimization algorithms have the defects of high time complexity, high space complexity and low

robustness<sup>[19]</sup>. Especially, in the optimization process of the neural network algorithm, for example, for the ant colony algorithm in the optimization process of the RBF network, the convergence speed is too slow at the beginning of the operation, which makes the time complexity of the RBF network increase, which is not conducive to the RBF network in the furnace flame detection. In addition, by comparing the performance of other swarm optimization algorithms, PSO algorithm is selected to optimize the flame detection model based on RBF neural network. The optimization process is shown in Fig. 2.

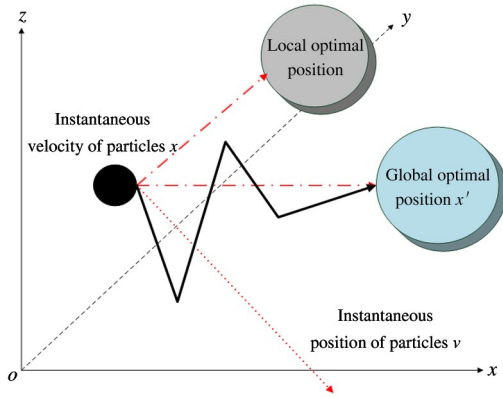


Fig. 2 PSO optimization process diagram

This paper uses PSO algorithm to optimize the structure of the RBF neural network. As shown in Fig. 2, each particle in the PSO algorithm dynamically updates its velocity  $v$  and position  $x$  with the individual optimal value and the global optimal value. By adjusting the position of each particle to obtain its own optimal result and the optimal value of neighboring particles, the global optimal position  $x'$  can be obtained.

In the  $n$ -dimensional space, the position vector and velocity vector of the  $i$ th ( $i = 1, 2, \dots, n$ ) particle are expressed as  $x_i = (x_{i1}, x_{i2}, \dots, x_{in})$  and  $v_i = (v_{i1}, v_{i2}, \dots, v_{in})$ . The expression process of the algorithm is shown as

$$x_{in}(t+1) = x_{in}(t) + v_{in}(t+1) \quad (1)$$

$$v_{in}(t+1) = \omega v_{in}(t) + c_1 r_1(t) [p_{in}(t) - x_{in}(t)] + c_2 r_2(t) [p_{gn}(t) - x_{in}(t)] \quad (2)$$

As shown in Eq. (2),  $v_{in}(t+1)$  represents the velocity of the  $i$ th particle when the time is  $(t+1)$  in the  $n$ -dimensional space, and the value range is  $[-v_{\max}, v_{\max}]$ ,  $p_{in}(t)$  is the currently obtained individual optimal position,  $p_{gn}(t)$  is the currently obtained global optimal position,  $\omega$  is the inertia weight value that controls the influence of the previous speed on the current speed,  $c_1$  and  $c_2$  are the acceleration coefficient (adjust the state and trajectory of particle movement in space by adjusting the values of  $c_1$  and  $c_2$ ),  $r_1(t)$  and  $r_2(t)$

are two independent random numbers uniformly distributed in the range of  $[0, 1]$ .

During the optimization process, the particles will still change near the optimal solution, which will cause deviations in the final optimization result. Therefore, the inertia weight value is iteratively updated to make the optimization result approach the optimal position. The iterative algorithm is shown in Eq. (3).

$$\omega = \omega_{\max} - \left[ \frac{2 \cdot iter}{iter_{\max}} - \left( \frac{iter}{iter_{\max}} \right)^2 \right] \times (\omega_{\max} - \omega_{\min}) \quad (3)$$

Same as in Eq. (1),  $\omega$  is the inertia weight value that controls the influence of the previous speed on the current speed,  $iter$  represents the number of iterations of the algorithm, and  $iter_{\max}$  represents the maximum number of iterations.

### 1.3 Design of PSO-RBF flame detection model

In the design of the PSO-RBF flame detection network, the improved particle swarm algorithm is used to obtain important parameters such as the neuron center  $c_m$  in the hidden layer of the RBF flame detection network, the width of the function  $\delta_i$ , and the output connection weight value. In this way, the training accuracy of the network is improved, so that the global optimal solution can be found in a short number of iterations of the particle swarm algorithm. When the algorithm iterates, the parameters of the RBF flame detection neural network are used as the optimization variables of the particles. Moreover, the root mean square error (RMSE) function in the RBF flame detection neural network is selected as the fitness function of the particle swarm algorithm.

In the RBF flame detection neural network, the parameter setting needs to be done in each layer of the hidden layer and each stage of the output layer. The RBF neural network parameter is used as the particle space position, and the position parameter is shown as

$$a_i(1, 2, \dots, i) \quad (4)$$

Each parameter of the hidden layer has a corresponding output value, and  $m$  is used to represent the output value of the  $m$ th neuron, as shown in Eq. (5).

$$\varphi_m(x) = e^{-\frac{\|x - c_m\|}{\delta_m^2}} \quad (5)$$

where  $\delta_m$  is the width of the function, and  $c_m$  is the center value. Therefore, the output value of the output layer of the network can be obtained as Eq. (6).

$$y = \sum_{m=1}^m \omega_m \varphi_m \quad (6)$$

Among them, the final network output value is represented by the summation value of the product of the output value  $\varphi_m$  of the  $m$  neurons in the hidden layer

and the inertia weight value  $\omega_m$ . In the process of training and adjusting parameters, it is necessary to adjust and optimize the network structure and parameters at the same time. The number of neurons in the hidden layer  $m$  and the size of the parameters will directly affect the performance of RBF neural network.

In addition, in order to better balance the training accuracy and structural complexity of the RBF neural network, the network has better generalization ability, the particle fitness function is shown as Eq. (7).

$$f(a_i(t)) = \beta D_i + Er_i(t) \quad (7)$$

In Eq. (7), the  $\beta$  parameter represents the balance factor, and its value is always positive; and  $D_i$  represents the number of parameters of the  $i$ th particle, which directly affects the time complexity of the flame detection model and affects the efficiency of the flame detection system. Its expression is shown in Eq. (8).

$$D_i = \begin{cases} D_i - 1 & D_i > D_{\max} \\ D_i + 1 & D_i \leq D_{\max} \end{cases} \quad (8)$$

When the value of  $D_i$  is greater than the maximum parameter  $D_{\max}$ , its value will increase by 1 unit, otherwise it will decrease by 1, where  $D_{\max}$  is also the parameter value of the optimal particle.  $Er_i(t)$  represents RMSE, and its expression is shown as Eq. (9).

$$Er_i(t) = \sqrt{\frac{1}{T} \sum_{t=1}^T [y(t) - y_e(t)]^2} \quad (9)$$

where,  $T$  is the number of data samples,  $y(t)$  and  $y_e(t)$  represent the actual output and expected output of the neural network, respectively. The particles in the space are continuously optimized to realize the optimization and parameter adjustment of the RBF flame detection neural network. The optimization process of the network is shown in Fig. 3.

**Step 1** Select the initial particle at the center of the radial basis function in the RBF neural network, randomly generate the initial particle composed of the RBF parameters  $\tau$  and  $c$ , and then set the PSO parameters, including the population size  $s$ , the maximum number of iterations  $iter_{\max}$ , and the inertia weight  $\omega$ , learning factors  $c_1, c_2$ .

**Step 2** Calculate the fitness. Evaluate the fitness value of each particle, i. e., verify the average classification accuracy. The current particle is taken as its individual optimal point, and the particle with the largest fitness value is taken as the global optimal point.

**Step 3** Update the velocity and position of each particle separately. Evaluate the current fitness of each particle and compare the fitness value with the fitness value of the individual optimal point and the global optimal point. If the current value is better, update the current value to the particle's individual optimum or

global optimum.

**Step 4** Check stop criteria. If the maximum number of iterations is reached, the evolution process will be stopped. Otherwise turn to step 3.

**Step 5** Determine the parameters. When the maximum number of iterations is reached and the stopping criterion is satisfied, the optimal parameters  $\tau$  and  $c$  are finally obtained. Then, end the training and validation process and build the PSO-RBF model.

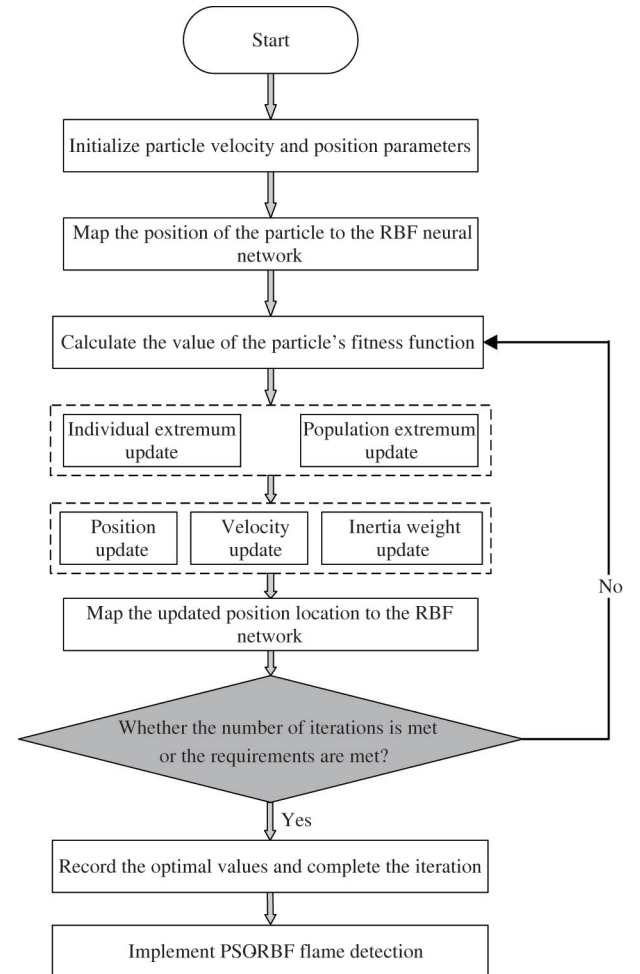


Fig. 3 Flow chart of PSO-RBF flame detection algorithm

## 2 Training and testing of PSO-RBF network

The flame detection algorithm design, training and testing process based on RBF neural network and PSO-RBF neural network are all carried out in Matlab R2022a, and the network environment parameters are shown in Table 1.

### 2.1 Processing of flame data samples

In this paper, continuous flame video data is used as input data, but the video data needs to be dimensionally reduced to convert the three-dimensional video

Table 1 Experimental environment and software version

Experiment hardware environment and software version description	
Operating system	Windows 11
CPU	Intel(R) Core(TM) i7-12700H CPU@ 2.3 GHz
RAM	16 GB
Matlab version	R2022a

information into continuous images, and the flame image acquisition frequency of 6 Hz is used. The flame state information at time  $t - 1$  and time  $t + 1$  is compared with the flame at time  $t$ , and the time interval is  $1/6$  s. Fig. 4 shows the flame image sample when the sampling interval is  $1/6$  s.

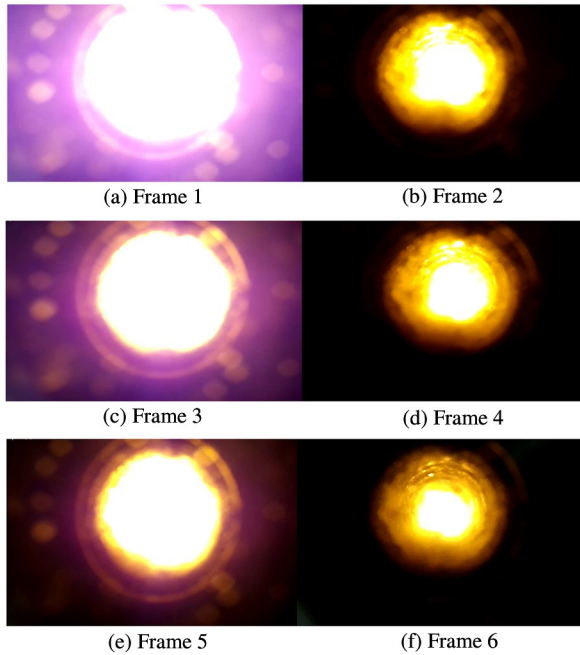


**Fig. 4** The changing state of the flame image when the sampling frequency is 6 Hz

Fig. 4(a) – (f) correspond to the 6 flame images collected under the sampling time length of 1 s. It can be seen that the flame in Fig. 4(a) is generated due to the change of fuel in the furnace. In the case of flickering, Fig. 4(b) clearly shows the normal combustion state of the flame, that is, the flame is yellow. Fig. 4(c), (e) are still the flames in the flickering state, but it can be clearly seen that the brightness of the flame flicker is gradually decreasing, and the flame is stabilizing. Combined with the change period of Fig. 4(a) – (f), the image sampling frequency of 6 Hz used in this experiment can capture exactly 3 flickering change periods of the flame within 1 s, that is to say, at  $1/6$  s the time interval is sampled, and the change

information of the flame can be recorded in each captured image and the image data of the adjacent time series.

For the preprocessing of the data set, sampling is performed by means of video frame processing. This paper uses a video of the flame state of the boiler furnace, and according to the flame state, intercepts a complete flame cycle as the original sample, including large fire, small fire, normal flame combustion, and the flame extinguishing stage. The video data is processed frame by frame to obtain a set of continuous furnace flame images. After grayscale processing and feature extraction, the flame area value of the sample data is calculated, and the area value is generated into a data matrix as the input of the network vector  $A$ . In the same way, by calculating the area of smoke in the image, taking the area of smoke in the image as input  $B$ , and inputting both sets of inputs into the PSO-RBF network for training, the size of the smoke generated by combustion in the furnace is obtained.

The referenced training sample data are shown in Table 2.

Table 2 Number of training samples

Types of flame samples	Training samples	Test samples	Total
Large flame	180	20	200
Medium flame	180	20	200
Small flame	180	20	200
Flame off	180	20	200

It can be seen from the training set and test set data in Table 2, the original number of samples of the flame area of the furnace is 800 intercepted flame images, including 200 samples for each of the four flame types, and the flame area value in the grayscale image is used as a sample to generate a four-dimensional array  $M$ , whose size is  $4 \times 200$ , and the  $M$  arrays are used as samples for training, 90% of which are used as training data sets and the remaining 10% are used as test data sets. The number of input samples for furnace smoke is 180, which is only used as an auxiliary measurement other than the detection of flame combustion state. The sample data is also obtained by processing the collected furnace smoke area. The experiments for furnace smoke detection are hereby used as reference comparison experiments.

## 2.2 Training and testing of the network

The parameters of the flame detection network are an important factor affecting the training and test results, so the parameters of the algorithm need to be ini-

tialized, the specific settings are shown in Table 3.

From Table 3, it can be seen that the specific parameters are set as follows, learning factor is  $c_1 = c_2 = 1.49$ ; initial inertia weight is  $\omega = 0.9$ , the inertia weight of the network when it reaches the maximum

number of iterations is 0.2, number of iterations (epoch) is 1000 times; population size is 10, width  $\delta$  is 1.2602, target error is 0.001, and sample input dimension is 4.

Table 3 PSO-RBF algorithm parameter settings

	Learning factor $c$	Initial inertia weight	Number of iterations (epoch)	Population size	Width $\delta$	Target error	Sample input dimension
PSO-RBF	$c_1 = c_2 = 1.49$	$\omega = 0.9$	1000	10	1.2602	0.001	4

The training and testing results of the RBF network are shown in Fig. 5. The output value of the network is normalized, and the output value range is  $[0, 1]$ . The four preset flame types are grouped, and the specific classification threshold is set as: the parameter range of the fire state is set to  $[0.8, 1]$ , this is because when the characteristics of the flame are the largest, its pixel area occupies approximately the entire 80% - 100% of the image. Similarly, set the sample parameter range of the normal combustion state of the flame to 40% - 80%, and the range of the small fire state in the furnace to be 20% - 40%. The judgment of the flame extinguishing state is based on the small fire state, that is, the area percentage is reduced to less than 20%, and the flame state is set to flame extinguishing when the continuous data shows a decreasing trend.

After completing the delineation of the training set and the test set, 200 sets of flame sample data were trained. After 1000 epoch iterations, the results shown in Fig. 5 are obtained. In the images of the training and test sets, the expected value of the flame sample is represented by the open circle, and the actual output value of the network is represented by the asterisk. It can be seen from the training result graph that among the flame training samples input to the network, the training accuracy of the RBF flame detection network is 81.0%, and 162 samples have realized the judgment of the flame type, but there are only 8 groups in the test samples. The sample achieved within-error classification. Judging by experience, the number of hidden nodes in the RBF network is modified under the condition that the network learning rate parameters and other settings are constant, but the test still does not meet the expected network accuracy requirements.

RBF network has the problem of insufficient accuracy in the process of training and testing. Therefore, the RBF flame detection neural network is further optimized by particle swarm algorithm.

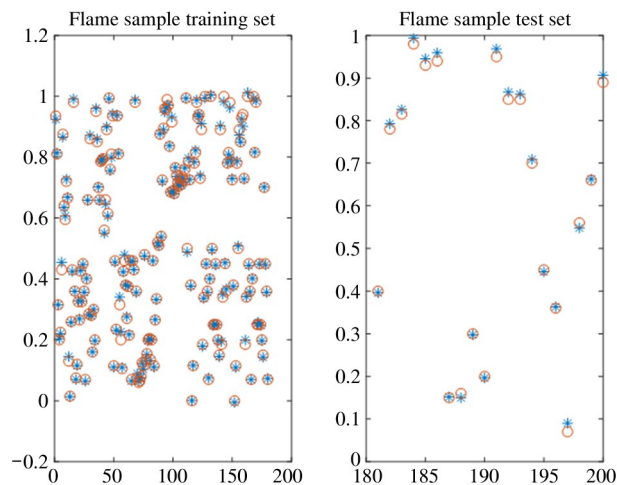


Fig. 5 RBF network flame detection training and testing results

Using a flame sample data matrix with a size of  $4 \times 200$ , the results shown in Fig. 6 are obtained after training. It can be seen that in the training process of the network, there are 19 groups of sample data expected values and actual output values. There is a certain training deviation, the final accuracy on this dataset is 90.5%. It can be seen from Fig. 6 that the data with large deviation in the classification results are mainly

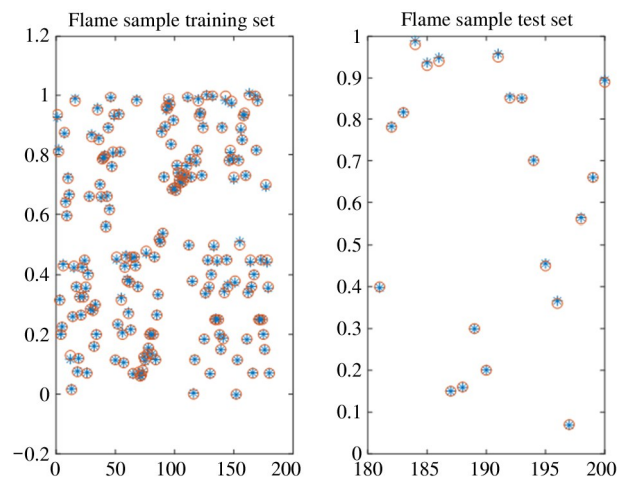


Fig. 6 PSO-RBF network flame detection training and testing results

distributed in the two intervals  $[0.3, 0.5]$  and  $[0.8, 1]$ . In the test phase of the network, 10% of the 200 sets of flame data were used as the test samples. After the algorithm iteration, 20 sets of classification results were obtained. Among them, the actual classification results of 4 sets of samples were quite different from the expected values. The distribution interval is also concentrated in the  $[0.3, 0.5]$ ,  $[0.8, 1]$  interval. Through the training and testing results of the network, it can be seen that the PSO-RBF flame detection network has obvious improvements in accuracy and fitting ability compared with the RBF flame detection network.

### 3 Experimental results and analysis

#### 3.1 Performance comparison and analysis

In the problem of flame detection in the boiler furnace, the final classification result is represented in the form of a matrix. For example, for the combustion state of the flame, the classification categories are the flame bright state, the normal flame burning state, the small fire state, and the flame extinguishing state categories, corresponding to the matrix form as the output results, namely  $[1,0,0,0]$ ,  $[0,1,0,0]$ ,  $[0,0,1,0]$ ,  $[0,0,0,1]$ , in which 1 in the definition array vector is the corresponding state of the flame, and 0 is the category with a smaller classification probability, this is because the output of the RBF network is classified by probability, for example, the probability that the flame state is bright reaches 80%, at this time, the probability that the flame state is judged to be bright is greater, and at the same time, the greater the probability of approaching the expected value is, the smaller the error value of classification is.

As shown in Fig. 7, the curve represents the change trend of RMSE in the unoptimized RBF network. The convergence interval in the figure can be divided into

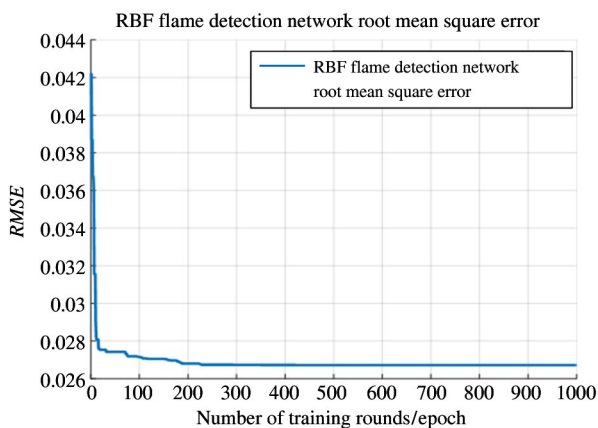


Fig. 7 RBF flame detection network mean square error

three parts. The fast convergence interval is taken as the first part, and the corresponding interval is  $[0,30]$  in the figure. The approximate convergence interval  $[30,229]$  is taken as the convergence change interval in the second part of the curve, the curve convergence speed of this part is lower than that of the fast convergence interval, but after the 229th epoch, the convergence of target error interval will become a stable convergence interval, and the error interval will stabilize between  $[0,0.001]$ , gradually approaching 0.026 as the number of training epochs increases.

The change curve of the root mean square error of the PSO-RBF flame detection network is shown in Fig. 8. It can be seen from the figure that the PSO-RBF network converges rapidly in the first 10 iterations, and converges to the 6th epoch. In the interval  $[0.0001, 0.001]$ , it converges to 0.0001 after 15 epoch iterations, the convergence speed is faster, and it is closer to the expected value.

Compared with the unimproved RBF network, the PSO-RBF network can achieve stable convergence in fewer training rounds, and the training error is smaller. It can also be seen that in the same network structure, PSO-RBF flame detection network has better convergence speed than RBF network.

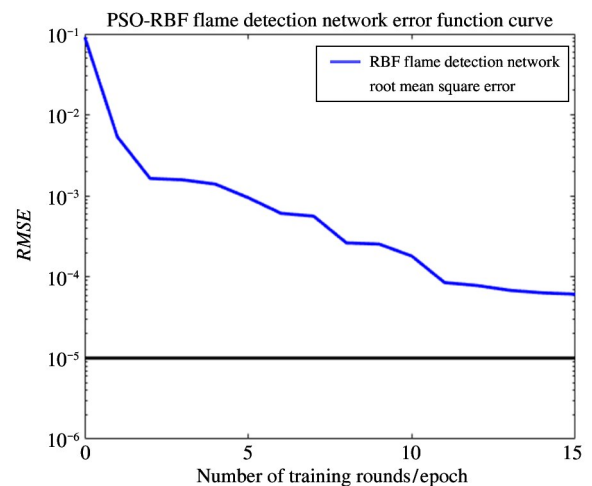


Fig. 8 PSO-RBF flame detection network mean square error

In addition, the real-time performance and accuracy of the algorithm are also particularly important in the flame detection system. The PSO-RBF network proposed has obvious improvements in RMSE value, convergence speed, and algorithm complexity of the algorithm. The specific performance comparison parameters are shown in Table 4.

It can be seen from Table 4 that when the number of neurons in the hidden layer is set to 6, the RMSE of the RBF flame detection network model optimized by

the PSO algorithm is 0.03, which is much smaller than the error of the RBF network of 0.092, and the running time of the algorithm is 15.2 s, which is nearly 1.7 s faster than the unoptimized RBF network; when the number of neurons in the hidden layer is set to 10, the RMSE of the PSO-RBF flame detection network is 0.008, although slightly higher than that of 6 neurons, but still far lower than the error of 0.054 of the RBF flame detection network. The algorithm running time at this time is 20.6 s, which is 8.3 s higher than that of the RBF network. For the small increase in the mean

square error, it is considered that the number of furnace flame samples when the number of neurons in the hidden layer is set to 15, the speed of using the PSO-RBF network is 6.6 s faster than the running time of the RBF network, and the RMSE is 0.013, which is higher than the convergence range of the RBF network. In summary, the flame detection model trained by the PSO-RBF network has higher performance than the unoptimized and improved RBF network, and the network can converge in a shorter time, so the algorithm is more efficient.

Table 4 PSO-RBF flame detection algorithm performance comparison

RBF				PSO-RBF			
Number of neurons	Target error <i>RMSE</i>	Algorithm execution time/s	Algorithm execution speed/fps	Number of neurons	Target error <i>RMSE</i>	Algorithm execution time/s	Algorithm execution speed/fps
6	0.092	16.9	177	6	0.03	15.2	200
10	0.054	28.9	103	10	0.008	20.6	140
15	0.042	33.2	90	15	0.013	26.6	110

### 3.2 Application verification of the algorithm

In order to verify the generalization ability of the PSO-RBF flame detection model in furnace flame detection, and to ensure the real-time detection, the continuous video signal collected from the boiler is selected as the input, the video\_reader function is used to read the flame video image, and the video samples are processed through frames images stored in time series. Finally, 3000 images in the flame change stage are cut out, and the sample array obtained after image grayscale, feature extraction, area, and frequency calculation is used as the input of the PSO-RBF network. The final test results are as follows.

As shown in Fig. 9, by using the data samples of 3000 flame images as input, the performance of the PSO-RBF network was tested for flame detection, and

the results of the flame state change were obtained, as shown in the curve in Fig. 9.

It can be seen from Fig. 9 that  $[0, 1]$  is used as the range of the flame area size, that is, the change process of the flame from extinguished to bright state. From the curve changes, it can be concluded that the flame in the furnace is initially in the image in the  $[0, 600]$  frame interval, due to the ignition of the furnace, the combustion supply changes during the process of adding fuel, so the flame flicker occurs, and the duration is about 10 s; when the flame is in the  $[600, 2400]$  frame interval, the change is basically stable, the average area percentage fluctuation difference is 0.18, and the overall trend of the flame is in a 'bright' state. However, the change from 'bright' to 'off' state occurred from 1500 to 1510 frames of images, this is because the flame is in the stable process, a change in the difference interval in the range of  $[0, 0.3]$  occurs, and the flame area at this time is reduced to the critical value of the 'off' state of the PSO-RBF network, so there is a misjudgment of about 1 s. On the whole, the determination of the flame in the combustion process is basically accurate. The flame image in the  $[2400, 3000]$  frame number interval fluctuated twice as a whole, this is because the flame 'extinguished' caused by the large flame flickering interval in the  $[2400, 2460]$  and  $[2750, 2800]$  frame number intervals judgment, subsequent adjustments can be made by increasing the sampling interval and adjusting the training weight parameters.

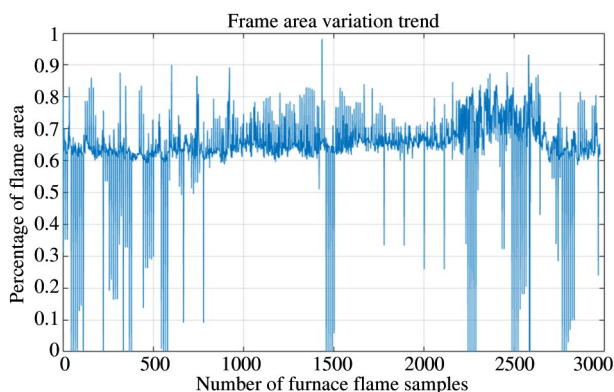


Fig. 9 Judgment result of boiler flame area

For the judgment of the flame smoke change in the

furnace, the flame image of the same time series as the flame state is used, and the smoke area parameter is taken as the input. The processing method of the algorithm is consistent, and the smoke change curve is obtained through the judgment of the PSO-RBF network, shown as Fig. 10. Since the inertia weight parameter in the initial training stage is set to 0.9, the detection accuracy of the flame state change is high, but the detection accuracy of smoke in the furnace is low. The smoke detection results in Fig. 10 are distributed in the range of  $[0.7, 1]$ , and the reason for the high smoke value mainly includes the interference factors of the reflection spectrum of the inner wall of the furnace in the flame sample. Therefore, the smoke detection adopts a high probability judgment method, that is, when the change value of the smoke area exceeds 0.75, the state in the furnace will be judged as 'smoke exists', and when the change range of the smoke area value is 0 to 0.75, it will be judged as 'no smoke' state.

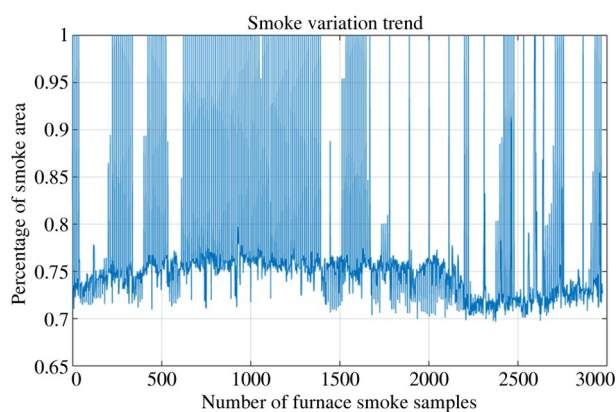


Fig. 10 Judgment result of boiler furnace smoke

The normalized interval  $[0, 1]$  corresponds to the state of smoke in the furnace from 'no smoke' to 'smoke present'. It can be seen from Fig. 10 that the change interval of the smoke area is  $[0.65, 1]$ . In the flame images from 0 to 300 frames, the flame is in the initial state of changing from 'off' and flickering to 'on', corresponding to the smoke detection judgment interval  $[0.7, 0.75]$ , and the smoke variation range is very small. At this time, according to the PSO-RBF network judgment, the output result is 'no smoke' state, that is, the furnace is in 'flame bright' and 'no smoke' state; it can be seen from the frame number interval of  $[700, 1390]$  that the range of the smoke area change area is  $[0.7, 1]$ , this part of the image corresponds to the 'bright' state of the flame in the stable stage in the flame detection experiment. At this time, when the flame is in the bright state, there is a certain amount of smoke in the furnace. According to the probability interval, it is judged that it is in the state of

'smoke exists'.

## 4 Conclusion

This paper takes the design of the RBF network as the basis. First, the initialization particle of the radial basis function center in the RBF neural network is selected, and the PSO algorithm is used to optimize the network and set the network parameters. Second, through the iterative update of the network, after obtaining the global optimal solution, the construction of the network model is realized. Last, the flame sample data obtained after feature extraction, area calculation, and frequency extraction of the original flame image through image processing algorithms are used as samples for training and testing of the PSO-RBF neural network. The experimental results show that the PSO-RBF flame detection network has a judgment accuracy of 90.5% in the case of fewer neurons, and has strong generalization ability, accuracy and fast convergence speed. Through the PSO-RBF network, the detection results of the flame state and the furnace smoke state in the furnace are used as a reference. On the whole, the performance of the flame detection algorithm described in this paper can basically meet the requirement of furnace flame detection of industrial boilers.

## References

- [ 1 ] ZHANG Q, YI H, YU Z, et al. Energy-exergy analysis and energy efficiency improvement of coal-fired industrial boilers based on thermal test data[J]. Applied Thermal Engineering, 2018, 144: 614-627.
- [ 2 ] HE X, ZHOU J H, LIAO Z H, et al. Research on flame classification and recognition based on object detection and similarity fusion[J]. The Journal of China Universities of Posts and Telecommunications, 2021, 28(5): 59-67.
- [ 3 ] KHAVANOV P. Research of heat transfer in reversible furnaces of low power boilers[C] // 2019 International Multi-Conference on Industrial Engineering and Modern Technologies (FarEastCon). Vladivostok: IEEE, 2019: 1-3.
- [ 4 ] MANSIR I B, RACHED B M. Oxy-fuel combustion in a two-pass oxygen transport reactor for fire tube boiler application[J]. Applied Energy, 2018(229): 828-840.
- [ 5 ] NEFEDEV A I, KONOVALENKO A A. Flame ionization detector for boiler control system[C] // 2020 International Conference on Industrial Engineering, Applications and Manufacturing (ICIEAM). Sochi: IEEE, 2020: 1-6.
- [ 6 ] HUANG J, LI S, CAI W, et al. Quantification of the size, 3D location and velocity of burning iron particles in premixed methane flames using high-speed digital in-line holography[J]. Combustion and Flame, 2021, 230: 111430.
- [ 7 ] ZHENG S, CAI W, ZHAO C, et al. On the measurement

- of flame temperature and emissivity based on multispectral imaging technique[J]. *Measurement*, 2022, 196: 1-11.
- [ 8 ] FAN R S, WANG Y, WEI D X, et al. Research on visual monitoring method of boiler furnace flame based on BP Neural Network [J]. *Computer Applications and Software*, 2015,32(2): 101-104. (In Chinese)
- [ 9 ] PARK M J, KO B C. Two-step real time night time fire detection in an urban environment using static ELASTIC-YOLOv3 and temporal fire tube[J]. *Sensors*, 2020, 20(8): 2202-2219.
- [10] JAGTAP H, BEWOOR A, KUMAR R, et al. Markov based performance evaluation and availability optimization of the boiler furnace system in coal fired thermal power plant using PSO [J]. *Energy Reports*, 2020, 6(3): 1124-1134.
- [11] HOSSEINI A, HASHEMZADEH M, FARAJZADEH N. UFS-Net: a unified flame and smoke detection method for early detection of fire in video surveillance applications using CNNs [J]. *Journal of Computational Science*, 2022, 61: 101638.
- [12] LI Z L, MIHAYLOVA L, YANG L. A deep learning framework for autonomous flame detection [J]. *Neurocomputing*, 2021, 448(5): 205-216.
- [13] CHAO X C, SHANG W, ZHANG F. Information-Guided flame detection based on faster R-CNN [J]. *IEEE Access*, 2020, 8: 58923-58932.
- [14] LV Z Y, JIA X W, YANG Y, et al. A comprehensive investigation of LSTM-CNN deep learning model for fast detection of combustion instability [J]. *Fuel*, 2021, 303: 121300.1-121300.14.
- [15] YU N, CHEN Y. Video flame detection method based on TwoStream convolutional neural network [C] //2019 IEEE 8th Joint International Information Technology and Artificial Intelligence Conference (ITAIC). Chongqing: IEEE, 2019: 482-486.
- [16] ASLAN S, GÜDÜKBAY U, TÖREYİN B U, et al. Deep convolutional generative adversarial networks for flame detection in video [C] //International Conference on Computational Collective Intelligence. Nagoya: IEEE, 2020: 807-815.
- [17] WEN Z, XIE L, FENG H, et al. Robust fusion algorithm based on RBF neural network with TS fuzzy model and its application to infrared flame detection problem [J]. *Applied Soft Computing*, 2019, 76(5): 251-264.
- [18] YE G Q, LI W G, HAO W. Study of RBF neural network based on PSO algorithm in nonlinear system identification [C] // The 8th International Conference on Intelligent Computation Technology and Automation (ICICTA). Nanchang: IEEE, 2015: 852-855.
- [19] CHEN Y X, LIAO X D, WANG J H, et al. Small image recognition classification based on random dropout and PSO-BP [C] // 2018 2nd IEEE Advanced Information Management, Communicates, Electronic and Automation Control Conference (IMCEC). Xi'an: IEEE, 2018: 1243-1246.

**WU Jin**, born in 1975. She received her B. S. degree from Xi'an Jiaotong University in 1998, and she also received her M. S. degree from Xi'an Jiaotong University in 2001. Her research focuses on key techniques for signal and information processing.